THE JOURNAL OF PHYSICAL CHEMISTRY B

Article

pubs.acs.org/JPCB

Influence of Hydrophobic Micelle Structure on Crystallization of the Photosynthetic RC-LH1-PufX Complex from *Rhodobacter blasticus*

Laurie-Anne Barret,[†,‡] Cherone Barrot-Ivolot,[†] Simon Raynal,[†] Colette Jungas,[‡] Ange Polidori,[†] and Françoise Bonneté*[,†]

[†]Institut des Biomolécules Max Mousseron (IBMM) UMR 5247 CNRS-Universités Montpellier 1 et 2, Chimie Bioorganique et Systèmes Amphiphiles, Université d'Avignon et des Pays de Vaucluse, 33 rue Louis Pasteur, F-84000 Avignon, France

[‡]CEA DSV IBEB Lab Bioenerget Cellulaire, CNRS UMR Biol Veget & Microbiol Environ, Aix-Marseille Université, Saint-Paul-lez-Durance, F-13108, France

ABSTRACT: Small angle X-ray scattering (SAXS) experiments are performed on two non-ionic surfactants, the dodecyl β-maltoside (DDβM) and the propyl(bi)cyclohexyl α-maltoside (PCCαM), a maltoside derivative containing a rigid bicyclohexyl group as hydrophobic chain, in order to compare the influence of both hydrophobic moiety structure and anomeric form on micelle form factors and intermicellar interactions relevant for membrane protein crystallization. Density and refractive index measurements were performed in order to determine volumetric and optical properties of surfactants, essential for determination of micelle molar masses by both SAXS and SEC-MALLS. SAXS form factors were analyzed by Guinier approximation and inverse Fourier transformation, to obtain the radius of gyration (R_G) and the pair distribution function ($P(r)$) of each surfactant. Form factor model fitting was also performed to describe the shape and the assembly of both surfactant micelles. Finally, second virial coefficients were measured at different percentages of polyethylene glycol 3350, in order to correlate surfactant intermicellar interactions and RC-LH1-PufX phase diagram. It is thus found that while size, shape, and dimensions of micelles are slightly similar for both surfactants, their molar mass and aggregation number differ significantly. PCCαM are more densely packed than DDβM, which reflects (1) an increase in van der Waals contacts between PCCαM hydrophobic chains in the micelle bulk and (2) a supplementary intermicellar attraction compared to DDβM. Finally addition of PEG, which induces a depletion attraction, decreases the solubility of the RC-LH1-PufX complex in PCCαM.

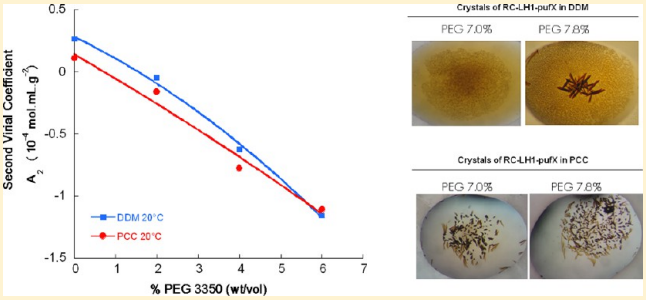

INTRODUCTION

Membrane proteins (MPs) play a fundamental role in biology as they are at the heart of all communications and transfers between the inside of living cells and their immediate environment. They represent roughly 30% of the proteome of *E. coli* or humans and 60% of current drug targets. Despite their importance in many cellular processes, knowledge of their structure and details of their molecular mechanisms remain sketchy at best—PMs represent about 2% of known structures in the Protein Data Bank. This lack of structural information is related to a number of difficulties: production of sufficient quantities, purification while conserving the structure/function/activity, and 3D crystallization for atomic resolution by crystallography. Regardless of how they are produced, MPs are usually purified using standard biochemical techniques, but require the use of detergents, surfactants which solubilize membrane lipids and make possible handling of membrane proteins in a hydrophobic environment. While increasing successes are obtained using *in meso* crystallization methods, i.e., by reconstitution in lipidic environment after solubilization and purification in detergents, growing high diffracting MP crystals directly in surfactant micelles—*in surfo*—a long-established method, remains a challenge in structural biology. Despite the use of high-throughput robotic platforms in combination with commercial or lab-made crystallization screens, crystallization by these trial-and-error methods is not frequently successful. Moving beyond empirical approaches requires a better understanding of the physics of these complex solutions containing both surfactant-solubilized MPs and surfactant micelles, whether it be for the supersaturation or the crystal growth step. In the 1990s, fundamental approaches have proven highly successful for the crystallization of soluble proteins.[1] Based on the study of interaction potentials between macromolecules in solution and second virial coefficient (A_2) measurements,[2,3] knowledge of crystallization mechanisms has progressed greatly thanks to a better understanding and control of physicochemical parameters that govern solution properties during supersaturation and crystal growth.[4] It has thus been shown that proteins crystallize in a regime where protein–protein interactions are attractive (or at least not strongly

Received: April 9, 2013
Revised: June 25, 2013
Published: June 27, 2013

repulsive). By using various model proteins (different structures, isoelectric point, size and compactness), we have shown that crystallization depends mainly on short- or medium-range attractions.[5−7] Salts induce an attractive term, which depends on the nature of anions and cations and follows either the direct or the inverse order of the Hofmeister series, depending on whether the protein is studied with a pH above or below its pI.[8−10] Other precipitants such as polyethylene glycol (PEG) induce a depletion attraction, which depends on the size and concentration of the polymer.[11] Recently, triblock amphiphilic polymers have also proven efficacious for soluble protein crystallization.[12] Whereas these amphiphilic polymers induce repulsion between soluble proteins at concentration below cmc (critical micelle concentration), increasing their solubility, they induce attraction at concentration above cmc, making protein crystallization possible. For membrane protein crystallization, interactions between surfactant micelles have also proven interesting. Results obtained with the integral membrane protein OmpF showed that characterizing interaction forces, via second virial coefficient measurements, between detergent micelles in the presence of crystallizing agents may be helpful to determine crystallization conditions for protein−detergent complexes (PDCs).[13−15] Berger et al. also characterized the phase behavior (consolute boundary and cloud point), micelle size, and second virial coefficient (PDC−PDC interaction) of the light-driven proton pump bacteriorhodopsin in β-octylglucoside.[16−18] In most cases, solution conditions that led to integral membrane protein crystallization fell within a similar range of negative A_2 values for detergent micelles and PDCs, suggesting that weakly attractive interactions are important in the control of membrane protein phase diagram, just as they are for soluble proteins. However, difficulties of MP crystallization remain essentially linked to the choice of detergent or surfactant type and concentration used to maintain the protein in a native folded state and the membrane protein−surfactant complex homogeneous, monodisperse, and stable for several days. Indeed the use of surfactants is ubiquitous and necessary in membrane protein biochemistry, in particular, to extract and solubilize proteins from membranes since it mimics the lipidic environment. Nature (polar head and hydrophobic chain) and concentration of surfactant are essential parameters to be controlled to optimize MP stabilization and crystallization. Surfactants in the presence of membrane proteins are under three forms in rapid equilibrium with one another: monomers, micelles, and surfactant bound to the protein, namely, the surfactant belt. Excess of protein-free surfactant micelles or excessively large surfactant belt may interfere with crystallization and crystal growth by preventing contacts between exposed polar surfaces.[19,20] Moreover, in crystallization methods such as vapor diffusion, the concentration step by concentrating both membrane protein−surfactant complexes and surfactant micelles may destabilize the protein by intrusion of alkyl chains in the membrane protein structure or by removing essential protein-bound lipids[21] or cofactors. To overcome these problems, different strategies have been developed for two decades to synthesize new surfactants, which make possible *in vitro* synthesis,[22,23] solubilization, and purification,[24,25] trapping, and stabilization[26] of membrane proteins. Most surfactants developed up to now are valuable for solubilizing and stabilizing MPs, while the number of effective surfactants for crystallization and X-ray crystallography studies is rather limited. Only rarely are new surfactants conceived, synthesized, and tested for membrane protein crystallization. Propyl(bi)-cyclohexyl α-maltoside (PCCαM) was deliberately designed to provide a more rigid environment for membrane protein crystallization, in order to improve the homogeneity of the protein−surfactant complex and its stabilization.[27] It is clear that a hydrophobic chain, which is less lipophilic for residual lipids and cofactors, less intrusive in transmembrane region of the protein, would probably be more favorable for crystallization by keeping MPs in their native form. Furthermore, new successful surfactants for crystallization are able to favor protein−protein contacts in the crystal. In order to better understand MP crystallization with new amphiphiles, we have studied the particular case of PCCαM by characterizing micelle structure and intermicellar interactions to know how it acts on the crystallization of a membrane protein of biological interest, the RC-LH1-PufX core complex from *Rhodobacter blasticus*.[28] Crystals of RC-LH1-PufX were previously obtained in a reproducible manner in PEG 3350 using dodecyl-β-maltoside (DDβM), a common detergent used in biochemistry for solubilization, purification, and stabilization of MPs because of its long alkyl chain. However, like most MP crystals obtained in DDβM, which diffract low to moderate resolution, RC-LH1-PufX crystals diffract in DDβM at low resolution of 8−10 Å at room temperature (Jungas, personal communication). This poor diffraction may be due (i) to a too large belt around the protein, which may prevent suitable polar−polar contacts in crystal for high diffraction, (ii) to the flexible, dynamic detergent micelle that surrounds the membrane protein, or (iii) to loss of cofactors due to intrusion of the long detergent alkyl chain, which destabilize the protein. The use of PCCαM, which possesses a rigid, less intrusive (bi)cyclohexyl group as hydrophobic part, could be an interesting method to obtain diffracting RC-LH1-PufX crystals. This surfactant has already been shown to be more stabilizing than DDβM detergent for some membrane proteins, such as the cytochrome b_6f complex from *Chlamydomonas reinhardtii* and two GPCRs.[27]

Our objective in this paper is to compare physicochemical properties of these two mild surfactants for membrane proteins, DDβM and PCCαM (Figure 1), and determine conditions for the growth of diffracting crystals. A thorough understanding of surfactant properties, structure, and interactions is essential for the determination of optimal conditions for membrane protein crystallization.

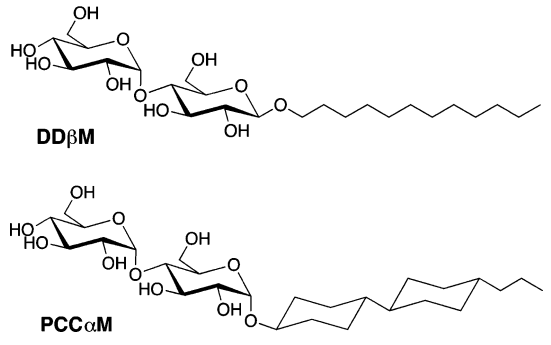

Figure 1. Chemical structure of dodecyl β-maltoside (DDβM) and propyl(bi)cyclohexyl α-maltoside (PCCαM).

EXPERIMENTAL SECTION

Solutions for Experiments. All salt and buffer reagents were purchased from Sigma Aldrich and polyethylene glycol

dx.doi.org/10.1021/jp403483q | J. Phys. Chem. B 2013, 117, 8770−8781

3350 monodisperse (50% w/v solution) was from Hampton Research. Dodecyl-β-D-maltoside (with percent α < 0.2%) was purchased from Affymetrix (Anatrace products). Propyl (bi)cyclohexyl-α-D-maltoside, the stable anomeric form, was synthesized at CBSA/IBMM (Avignon) following the protocol from Hovers et al.[27] For SAXS and SEC-MALLS experiments, all solutions were prepared with Milli-Q water, filtered on 0.2 μM Millipore filters.

RC-LH1-PufX Preparation. Dimeric RC-LH1-PufX complex was isolated from *Rb. blasticus* photosynthetic membranes according to the procedure described in Comeyras et al.[28] The protein solubilized in DDβM 0.015% was eluted from monoQ 5/50 GL column (GE Healthcare, Glattbrugg, Switzerland) with 20 mM Tris-HCl pH 8, DDβM 0.015%, NaCl 375 mM or with 20 mM Tris-HCl pH 8, PCCαM 0.01%, NaCl 375 mM in the case of surfactant exchange. Protein fractions were diluted with a Tris-surfactant buffer (at the same concentrations as elution buffer) to reduce salt concentration at 75 mM and concentrated to a final protein concentration ranging from 6 to 12 mg/mL.

Surfactant Phase Diagram and RC-LH1-PufX Crystallization Trials. Crystals of RC-LH1-PufX were grown by vapor diffusion (Linbro plates) at 20 °C with a reservoir solution containing 90 mM of $MgCl_2$, 10% of glycerol, and 5−10% of PEG 3350 in water. Crystallization drops were formed by mixing 1 μL of purified protein (6−12 mg/mL) with 1 μL of the reservoir solution. Surfactant phase diagrams were determined in 10 μL droplets of 6.5−10% PEG 3350 and 5−55 mg/mL surfactant in water using microbatch plates. For each PEG concentration, surfactant concentration was increased by 1 mg/mL step until obtaining a phase transition, observed by optical microscopy (Carl Zeiss SteREO Discovery.V12 microscope).

Density and Partial Specific Volume Measurements. Surfactant micelle partial specific volumes $\overline{v}_p$ in $cm^3.g^{-1}$ were calculated from the precise measurement, with a density-meter Anton Paar DMA4500M, of ρ and ρ°, respectively, the densities of surfactant solutions at different concentrations ranging from 0.1 to 10 $mg.mL^{-1}$ and H_2O. The stock surfactant solutions were prepared by precisely weighting both the surfactant and the solvent at about 10 $mg.mL^{-1}$. Surfactant solutions were obtained by successive dilutions from stock solutions. The partial specific volume was then obtained from the slope of the following expression:

$$\frac{\rho - \rho^\circ}{c} = 1 - \overline{v}_p \cdot \rho^\circ \tag{1}$$

Refractive Index and Refractive Index Increment Measurements. Surfactant micelle refractive index increments, $\partial n \partial c$ in $mL.g^{-1}$, were determined from the precise measurement, with an Optilab T-rEX refractometer from Wyatt Technology, of n the refractive index of surfactant solutions at different concentrations ranging from 0.1 to 5 $mg.mL^{-1}$ and analyzed with ASTRA V software (Wyatt Technology).

$$\frac{\partial n}{\partial c} = \frac{n - n_0}{c} \tag{2}$$

SEC-MALLS Analysis of Surfactant Micelles. Size exclusion chromatography coupled to multi-angle laser light scattering (SEC-MALLS) for absolute mass determination of surfactant micelles was carried out on a Shimadzu HPLC system using a silica gel BioSep 5 μm SEC-s2000 column (Phenomenex) coupled to an Optilab T-rEX refractometer and a miniDawn TREOS multi angle laser light scattering (MALLS) detector (Wyatt Technology). For each surfactant, the column was equilibrated, at a flow rate of 0.4 $mL.min^{-1}$ with Milli-Q water containing the surfactant at a concentration of 2 × cmc. Different concentrations of surfactant were injected.

Molar weight determination was performed with the ASTRA V software using the determined dn/dc values for each surfactant and the expression:

$$M_{mic} = \frac{\left(\frac{I_\theta}{I_0}\right)_{mic} - \left(\frac{I_\theta}{I_0}\right)_{buf}}{K\left(\frac{dn}{dc}\right)^2 (RI_{mic} - RI_{buf})} \tag{3}$$

with $K = [(2\pi^2 n^2)/(N_a \lambda^4)][(1 + \cos^2\theta)/(r^2)]$, an optical constant, which depends on the refractive index n of the buffer, λ the wavelength of the light, θ the angle between the incident (I_0), and the scattered light (I_θ), the distance r between the molecule and the detector and the Avogadro number.

SAXS (Small Angle X-ray Scattering). Synchrotron radiation X-ray scattering data were collected on the ID14-eh3 bioSAXS beamline at the ESRF (European Synchrotron Radiation Facility, Grenoble, France). Surfactant scattering patterns were measured at 293 K at several concentrations ranging from 2 to 40 $mg.mL^{-1}$ in H_2O with addition of different percentages of PEG 3350 (0%, 2%, 4%, and 6%). For the sample−detector distance of 2425 m and the X-ray wavelength λ = 0.0931 nm, the achievable q-range was 0.05−4 nm^{-1}. The beamline was equipped with a 2D detector (Pilatus 1M) and an automated sample changer. To prevent radiation damage during the scattering experiments, the data were collected in 10 successive 10 s-frames and the solution was moved in the capillary during exposure. The individual frames were averaged after normalization to the intensity of the incident beam and corrected for the detector response, and the scattering of the appropriate buffer was subtracted. The difference curves were scaled for the solute concentration. All data manipulations were performed using standard procedures by the program package PRIMUS.[29]

THEORETICAL SECTION

Form Factor. The total normalized intensity $I(c,q)/c$, scattered by a solution of interacting monodisperse particles at a scattering angle 2θ, can be expressed as a function of the particle concentration c and the modulus of the scattering vector $\mathbf{q}$, $\mathbf{q} = 4\pi\lambda^{-1} \sin\theta$, by

$$I(c, q) = I(0, q) \times S(c, q) \tag{4}$$

$I(0, q)$, the Fourier transform of the spherically averaged autocorrelation function of the electron density contrast associated with the particle, is usually called the particle form factor. $S(c, q)$, usually called the solution structure factor, is an interference term, which accounts for interactions between particles. From form factor analysis, we access different particle structural parameters. Using the Guinier approximation $\ln I(0, q) = \ln I(0, 0) - (qR_g)^2/3$, while assuming that $qR_g < 1$ at very small angles, the forward scattering intensity $I(0, 0)$ gives access to the particle absolute molar mass and the slope of the Guinier approximation to the radius of gyration R_g of the particle. The surfactant micelle molar mass was estimated from SAXS data by comparison of absolute forward scattering with that from the reference of a solution water.[30] The aggregation number N_{agg} is

dx.doi.org/10.1021/jp403483q | J. Phys. Chem. B 2013, 117, 8770−8781

therefore determined by dividing the micelle molar mass by that of the surfactant monomer by the following expression:

$$N_{agg} = N_a \frac{I(0)_{mic}}{M_{mono}(c - c_{cmc})I(0)_{water}[r_0 \cdot \bar{v}_p(\rho_{mic} - \rho\circ)]^2} \left.\frac{d\Sigma}{d\Omega}\right|_{water} \quad (5)$$

with N_a the Avogadro number, r_0 the classical electron radius ($r_0 = 0.28179 \times 10^{-12}$ cm/e$^-$), $\bar{v}_p$ the surfactant micelle specific volume (cm^3/g), $\rho_{mic}$and ρ^0, the scattering length density of surfactant micelle and water, respectively, and $(d\Sigma/d\Omega)|_{water}$ the absolute scattering intensity of water equal to 0.01632 cm^{-1} at 293 K.

By inverse Fourier transformation using the program GNOM,[31] the pair distribution function (PDF) and the maximum particle dimensions D_{max} can also be determined. It gives information about the geometrical shape of the particle in solution. Finally, the SAXS form factors can further be analyzed using least-squares models. Using SASfit software package,[32] a triaxial core shell ellipsoid model has been used to account for our experimental data. Its functional form is

$$I(q) = \int_0^1 \int_0^1 dx\, dy \left[3(\rho_{core} - \rho_{shell}) \frac{\sin qR - qR\cos qR}{(qR)^3} + 3(\rho_{shell} - \rho_{solv}) \frac{\sin qR_t - qR_t \cos qR_t}{(qR_t)^3} \right]^2 \quad (6)$$

with $R = \{[a^2\cos^2(\pi x/2) + b^2\sin^2(\pi x/2)](1 - y^2) + c^2y^2\}^{1/2}$

$$R_t = \{[(a + t)^2\cos^2(\pi x/2) + (b + t)^2\sin^2(\pi x/2)](1 - y^2) + (c + t)^2y^2\}^{1/2}$$

ρ_{core}, ρ_{shell}, and ρ_{solv} the scattering length densities of the core, the shell, and the solvent, respectively; a, b, and c three semiaxes of the elliptical core, and t the thickness of the shell. Volume of micelle core and total volume of micelle core along with shell can then be determined from these structural parameters

$$V_{core} = 4\pi/3(a\cdot b\cdot c) \quad \text{and} \quad V_{mic} = 4\pi/3(a + t)\cdot(b + t)\cdot(c + t) \quad (7)$$

By assuming no hydration of hydrophobic chain, the core volume determination appears to be another way to access the aggregation number by the expression $V_{core} = N_{agg} V_{chain}$. Finally, hydration of polar head can be determined by the expression $V_{shell} = N_{agg}(V_{head} + nV_{H2O})$, with $V_{head} = V_{monomer} - V_{chain}$.

Second Virial Coefficient Determination. In the case of nonideal solutions of macromolecules (i.e., concentrated solutions of macromolecules in interaction), the scattered intensity $I(c, q)$ gives information about microscopic properties between particles in solution via the structure factor $S(c, q)$. Forward structure factors, $S(c, 0)$, give access to the second virial coefficient A_2, which characterizes the resultant force of all individual interactions between particles in solution. These individual interactions are either repulsive or attractive. Mainly, these are the van der Waals forces, the excluded volume forces, the electrostatic forces, the hydration forces, and sometimes additional forces such as depletion forces when polymers are added. The nature of net interaction forces, either attractive or repulsive, can be simply determined by the plot of the structure factor at the origin, $S(c, 0)$, as a function of the particle concentration, c, since it is related to the osmotic pressure Π by

$$S(c, 0) = \frac{RT}{M}\left(\frac{\partial\Pi}{\partial c}\right)^{-1} \quad (8)$$

$$\text{with} \quad \frac{\Pi}{cRT} = \frac{1}{M} + A_2c + A_3c^2 + \ldots \quad (9)$$

the concentration c being expressed in g.cm^{-3}.

Therefore, the second virial coefficient can be obtained by the expression

$$S(c, 0) = \frac{I(c, 0)}{I(0, 0)} = \frac{1}{1 + 2\cdot M\cdot A_2\cdot c + \ldots} \approx 1 - 2\cdot M\cdot A_2\cdot c \quad (10)$$

In the case where the term $(2MA_2c)$ is small ($\ll$1), the expansion in power of c of the structure factor at the origin $S(c, 0)$ can be limited to the second virial coefficient and linearized. If A_2 is positive (negative), $S(c, 0)$ is less (greater) than 1, the overall interactions are repulsive (attractive).

RESULTS AND DISCUSSION

Surfactant Structure and Properties in Water. Surfactants are amphiphilic molecules, which contain both a polar hydrophilic head and a hydrophobic tail. In aqueous solutions, they form self-assemblies such as micelles, vesicles, bilayers, whose size and shape depend on the surfactant structural parameters,[33,34] such as its head area, its aliphatic chain length, its anomeric form for glycosylated surfactants or its apolar chain hydrophobicity. DoDecylMaltoside presents two anomeric forms, whose β form is the most frequently used in biochemistry as detergent to solubilize lipidic membranes and extract and stabilize membrane proteins for structural studies. Propyl(bi)cyclohexyl maltoside presents also two anomeric forms; however, the α form is the predominant stereoisomer obtained during its synthesis.[27] Shape and size of DDM micelles were already studied by small angle scattering.[35−37] The α-anomer forms spherical micelles, while the β-anomer forms large oblate ellipsoid micelles. We have performed SAXS experiments on both DDβM and PCCαM in H_2O at 20 °C on the same SAXS beamline over a large q-range, from 0.05 to 4 nm^{-1} (ID14-eh3, ESRF Grenoble-France), in order to compare the effect of hydrophobic chain structure and anomeric form on micellar assemblies and interactions for membrane protein crystallization, and in particular for RC-LH1-PufX crystallization. X-ray scattering intensities have been measured as a function of surfactant concentration between 2.5 and 40 g·L^{-1} widely above critical micelle concentration (cmc = 0.087 g/L and 0.02 g/L for DDβM and PCCαM, respectively) for both form factor characterization and second virial determination. Because of the very low signal of surfactant at concentration at and below cmc, similar to buffer signal, the subtracted background was the signal of water or of buffer. No change in the shape of scattering curves of surfactant micelles as a function of surfactant concentration is observed over the whole q-range for DDβM and for PCCαM (Figure 2), except slight changes in the zero-q

dx.doi.org/10.1021/jp403483q | J. Phys. Chem. B 2013, 117, 8770−8781

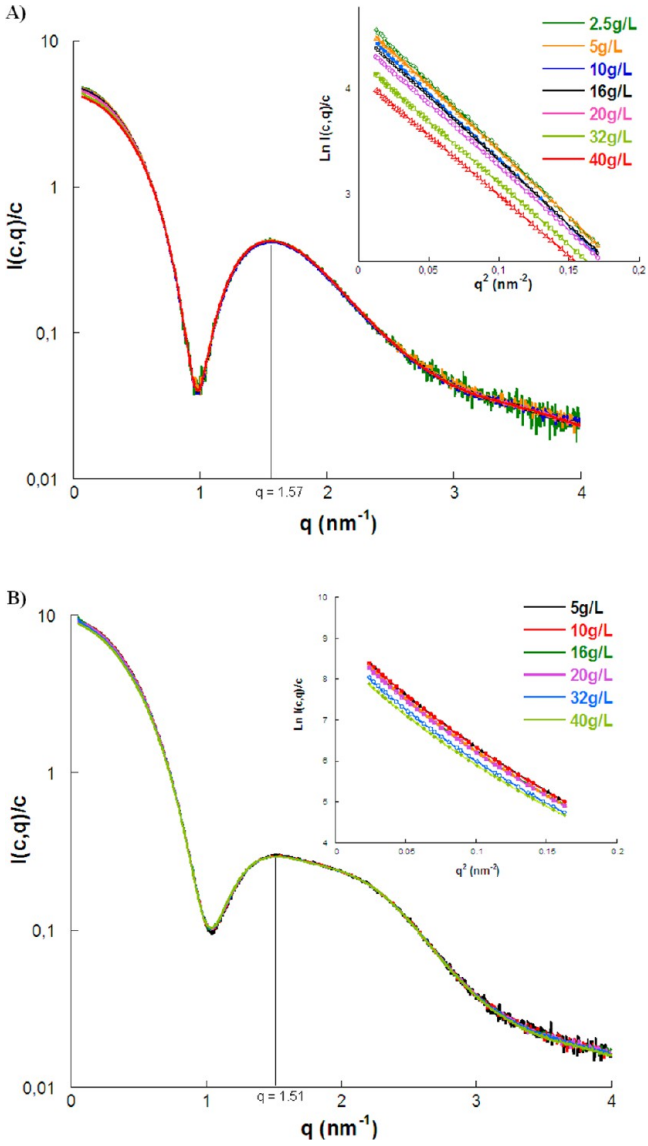

Figure 2. SAXS patterns of DDβM (A) and PCCαM (B) in H_2O as a function of concentration of each surfactant from 2.5 to 40 g/L.

range, corresponding to the interference term $S(c, q)$ (eq 4). A slight decrease in the position of the second maximum is observed for PCCαM, which could be attributed to a slight increase in the micelle size.[36] Around the first maximum, i.e., $q = 0$, the decrease in Ln $[I(0)/c]$ seen in Guinier plots as the surfactant concentration increases (inset Figure 2) is characteristic of repulsive interactions arising mainly from excluded volume effects.

In order to overcome interparticle effects on the molar mass and radius of gyration determination, form factors are taken as the most diluted concentrated SAXS curves for the Guinier analysis.[38] By the Guinier approximation, the forward intensity gives access to the micelle molar mass and thus to the surfactant aggregation number N_{agg} (i.e., the number of surfactant monomers per micelle) (eq 5). Forward intensity $I(0)$ and radius of gyration (R_G), listed in Table 1, are together higher for PCCαM than for DDβM. Molar mass and aggregation number for DDβM calculated from $I(0)$ are found in agreement with values from literature[39,40] between 110 and 140 for N_{agg}. For PCCαM, molar mass and aggregation

Table 1. Surfactant Properties

Surfactant (abbreviation)	DDβM	PCCαM
formula	$C_{24}H_{46}O_{11}$	$C_{27}H_{48}O_{11}$
total number of electrons	278	298
head number of electrons	181	181
chain number of electrons	97	117
formula weight (Da)	510.60	548.66
cmc (mM/g·L^{-1})	0.17/0.087	0.036/0.019
$\bar{v}_p$ (cm^3.g^{-1}) from density measurement	0.819	0.799
$\frac{\partial n}{\partial c}$ (mL.g^{-1})	0.143	0.160
$V_{monomer}$ (Å^3) from density measurement	694.3	727.8
V_{head} (Å^3) from chemical formula	344.1	344.1
V_{chain} (Å^3) from chemical formula	350.2	383.7
ρ^{elect} (e$^-$/Å^3) from density measurement	0.400	0.409
ρ^{elect} (e$^-$/Å^3) for polar headgroup	0.526	0.526
ρ^{elect} (e$^-$/ Å^3) for hydrophobic chain	0.277	0.305
ρ^{elect} (e$^-$/ Å^3) for H_2O = 0.334		
$I(0)$ (cm^{-1}) for 1% surfactant	0.247	0.426
M_w (kDa) SEC MALLS	65 ± 3	90 ± 1
M_w (kDa) SAXS	63 ± 0.5	89 ± 0.5
N_{agg}	124−131	163−166
R_G (nm) SAXS	3.2	3.3
D_{max} (nm) SAXS	8.0	9.0

number are found significantly higher than for DDβM. Results for M_w and N_{agg} were confirmed by SEC-MALLS analysis.

Figure 3 shows the elution profiles for two samples of each DDβM and PCCαM through a BioSep-SEC-s2000 column equilibrated in water containing their respective surfactant at a concentration of twice cmc in order to maintain surfactants self-associated in micelle form during elution. Solutions of each surfactant at two excess concentrations, i.e., largely above cmc (between 3 and 6 g/L) were injected and their static light scattering signals analyzed. From measured refractive index increments, $\partial n \partial c$, DDβM and PCCαM molar masses calculated from eq 3 and indicated in Figure 3 by the blue/green and red/magenta lines, respectively, are found close to the values obtained from SAXS measurements (see Table 1) and higher for PCCαM than for DDβM. Micelles for both surfactants appear monodisperse in mass along the elution peak. The effect of concentration for both surfactants on elution peak is simply due to the saturation of column pores at high concentration of surfactant.

Other structural information is obtained from SAXS analysis. The pair distribution function (PDF), $P(r)$, obtained by inverse Fourier transformation of SAXS intensity gives information on the shape and geometry of the particle and its maximum dimension (D_{max}). It has the advantage to be a free-model method, only depending on scattering length density profile into the particle.

We thus observe (Figure 4) a slight increase in D_{max} for PCCαM micelles compared to DDβM micelles, in agreement with the slight shift of the second maximum of SAXS intensity toward lower q. In both cases, $P(r)$ shows two peaks, but less marked for PCCαM than for DDβM. This behavior observed in the PDF is due to an inhomogeneous composition of particles. The scattering length densities of head and tail groups in micelles of DDβM and PCCαM (Table 1) are respectively higher and lower than that of the solvent for both surfactants. Thus, the hydrophobic core has a negative length density contrast and the hydrophilic shell has a positive contrast, which

dx.doi.org/10.1021/jp403483q | J. Phys. Chem. B 2013, 117, 8770−8781

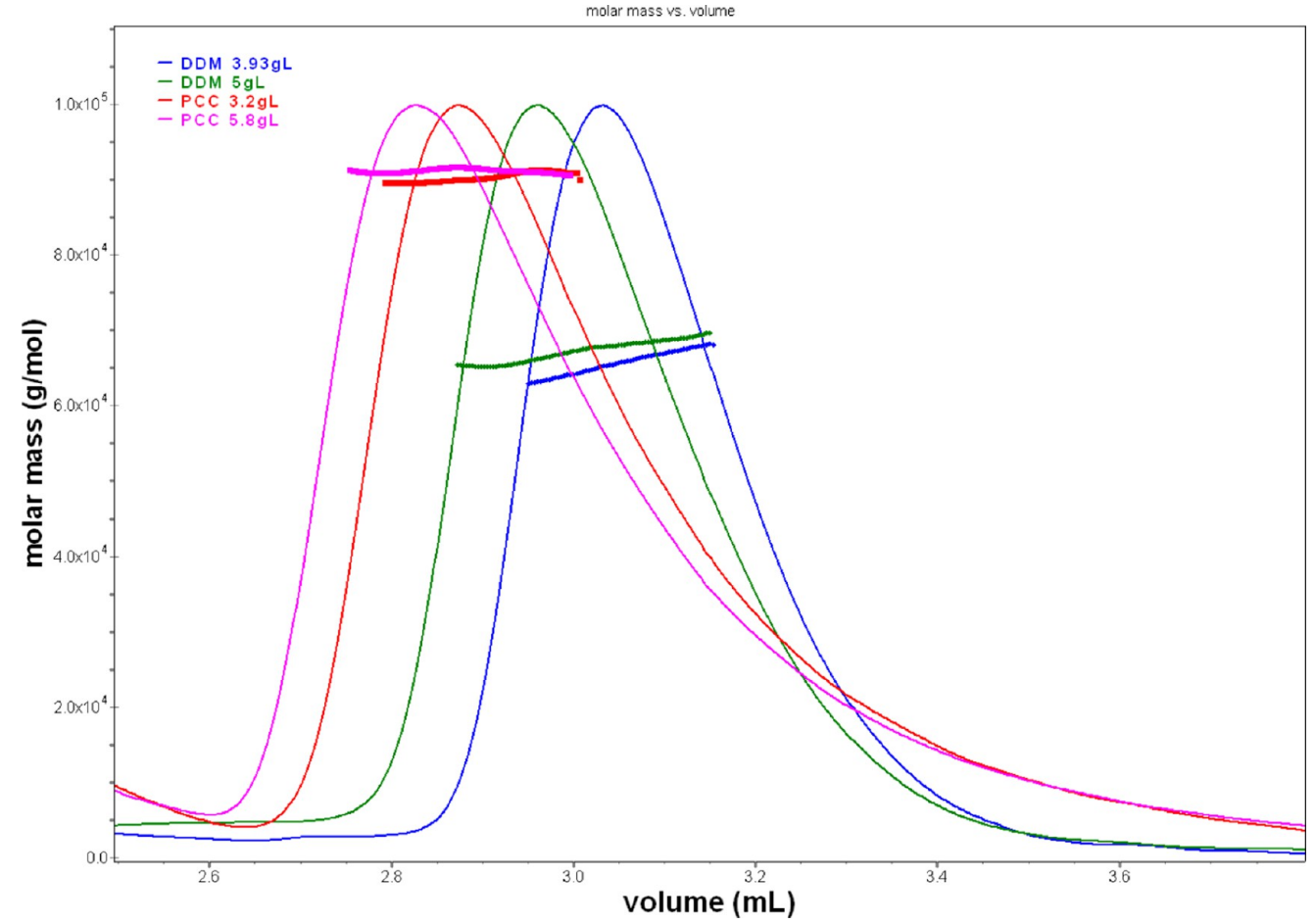

Figure 3. Gel permeation chromatogram coupled to triple detection UV-RI-MALLS from Wyatt technology.

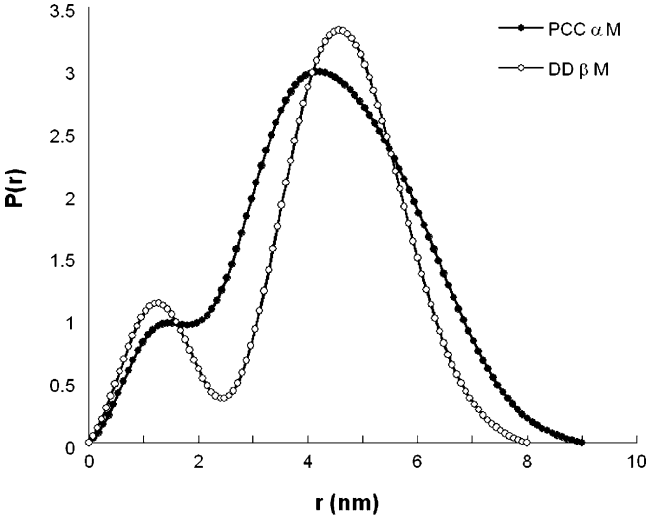

Figure 4. Pair distribution function of DDβM and PPCαM in water.

induces oscillations in the $P(r)$.[41] Evaluated by SAXS, the $P(r)$ function shows that a core−shell model could describe these micelles well. Fitting analysis of SAXS data was performed using an ellipsoid core−shell model. Such a simplistic model was already used to describe different detergent micelles[36] and appeared suitable to provide a comprehensive picture of micelle structure. In the SASfit procedure, assuming that the core contains no water molecules, the electron density for the core was kept fix to the calculated value obtained from the total number of electrons in the chain divided by the volume of the chain. For the shell electron-density, the value was not fixed, allowing hydration of the headgroup. Experimental and fitted scattering curves are shown in Figure 5. Keeping in mind that final model parameters, although strongly dependent on the choice of geometrical model, also depend on the experimental q-range and accuracy of collected data, we analyze data with two ellipsoidal models: (i) an oblate ellipsoid with one semiaxis of length a, two semiaxes of length b, and a thickness t for the head length as in Lipfert et al.;[36] (ii) a triaxial core−shell ellipsoid with semiaxes $a < b,c$ and thickness t as in Bauer et al.[42] This latter model fits intensities better than the biaxial model (Table 2), in the zero-q range which is larger than previous published experiments, mainly due to improvement in data acquisition detector, reflecting the forward intensities from Guinier analysis and therefore the micelle molar masses (inset in Figure 5) and the aggregation number.

Moreover, the hydrophobic micelle core volume, $V_c = 4\pi abc/3$, obtained from the ellipsoid model also provides an independent value of the aggregation number. Assuming that micelle core does not contain water molecules,[33] the micelle core volume can be written as $V_{core} = N_{agg}.V_{chain}$. The volume of the DD$\beta$M aliphatic chain, V_{chain}, was calculated from the Tanford method[33] using $V_{chain} = 27.4 + 26.9\ n_c$, with n_c the number of carbon atom ($n_c = 12$ for DDβM). Thus, N_{agg} for DDβM is found equal to 137 in close agreement with the value obtained from our Guinier analysis ($N_{agg} = 127 \pm 4$). For

dx.doi.org/10.1021/jp403483q | J. Phys. Chem. B 2013, 117, 8770−8781

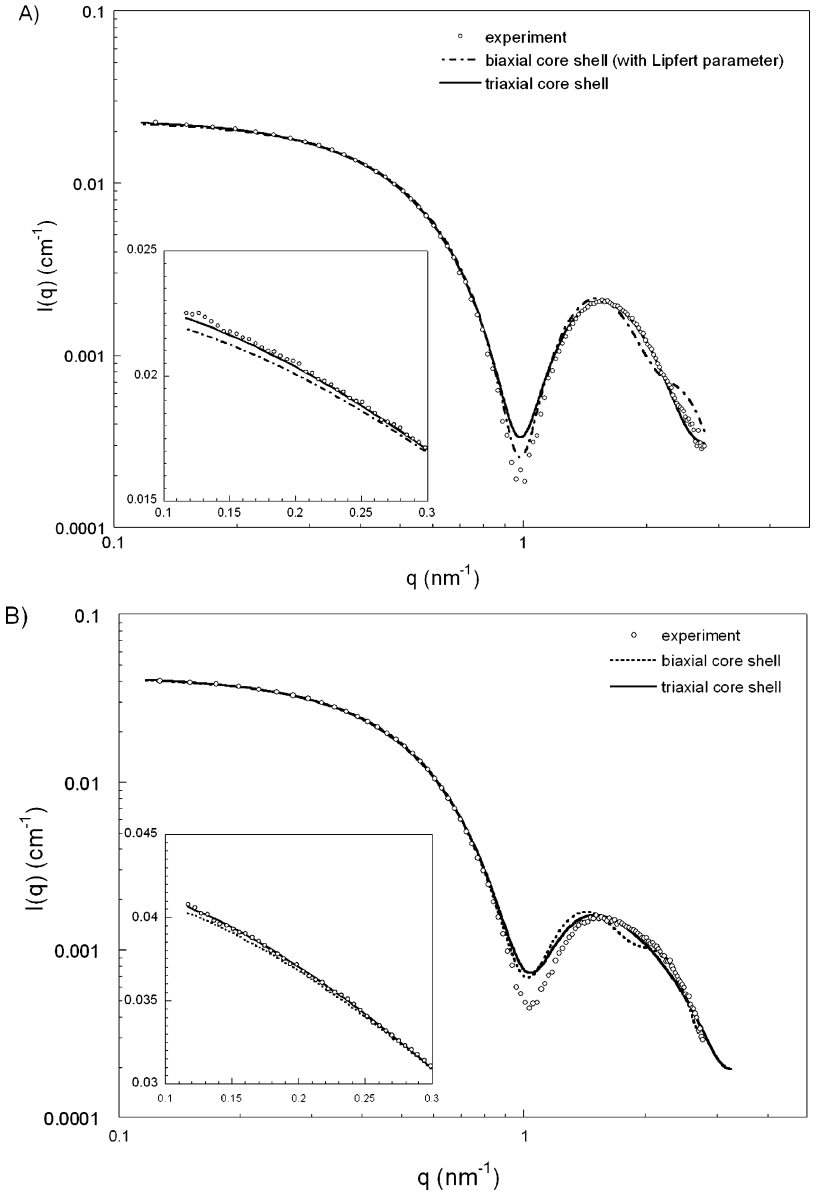

Figure 5. Experimental and fitted form factors of DDβM and PCCαM.

Table 2. Best Parameters from Triaxial Ellipsoid Fits

surfactant	shape	ρ_{shell} (e^-/A^3)	ρ_{core} (e^-/A^3)	a (A)	b (A)	c (A)	t (A)	V_c (A^3)	V_t (A^3)
DDβM	Oblate	0.446	0.277	15.26	22.02	34.08	8.35	47968	127439
PCCαM	Oblate	0.438	0.305	13.98	25.93	37.55	8.27	57017	146049

PCCαM, N_{agg} from core−shell model is found equal to 149 larger than DDβM, but quite a bit smaller than N_{agg} from Guinier forward intensity ($N_{agg} \approx 165$). This discrepancy is probably due to a SAXS fit of lower quality at large angles than for DDβM. From our fit, we could also evaluate the solvation of DDβM and PCCαM at around, respectively, 9 and 8 water molecules per maltoside head in agreement with literature.[35] Finally, our results clearly show that the PCCαM micelle, with size and hydration quite similar but aggregation number higher than DDβM, is denser than DDβM, which explains the shape of the two $P(r)$ and should influence the intermicellar interactions.

Intermicellar Surfactant Interactions. We have shown that DDβM and PCCαM exhibit quite similar micellar structures in aqueous solution. They can be described as oblate ellipsoids with equivalent dimensions (R_G, D_{max}), however with a larger aggregation number for PCCαM than for DDβM, which means that PCCαM is denser than DDβM. In H_2O, the scattering intensity at zero-q, for both DDβM and PCCαM, decreases as the micelle concentration of surfactant increases from 2.5 to 40 $g \cdot L^{-1}$ (inset Figure 2). The decrease in the case of DDβM is more pronounced than in the case of PCCαM. This decrease close to zero-q, without change in the large q-range up to 4 nm^{-1}, is characteristic of repulsive interaction between micelles. Structure factors at zero-q, $S(c, 0)$, have been plotted as a function of micelle concentrations for DDβM (Figure 6A) and PCC-αM (Figure 6B) in different solutions containing various percentages of polyethylene glycol 3350 from 0% to 6% (w/v).

dx.doi.org/10.1021/jp403483q | J. Phys. Chem. B 2013, 117, 8770−8781

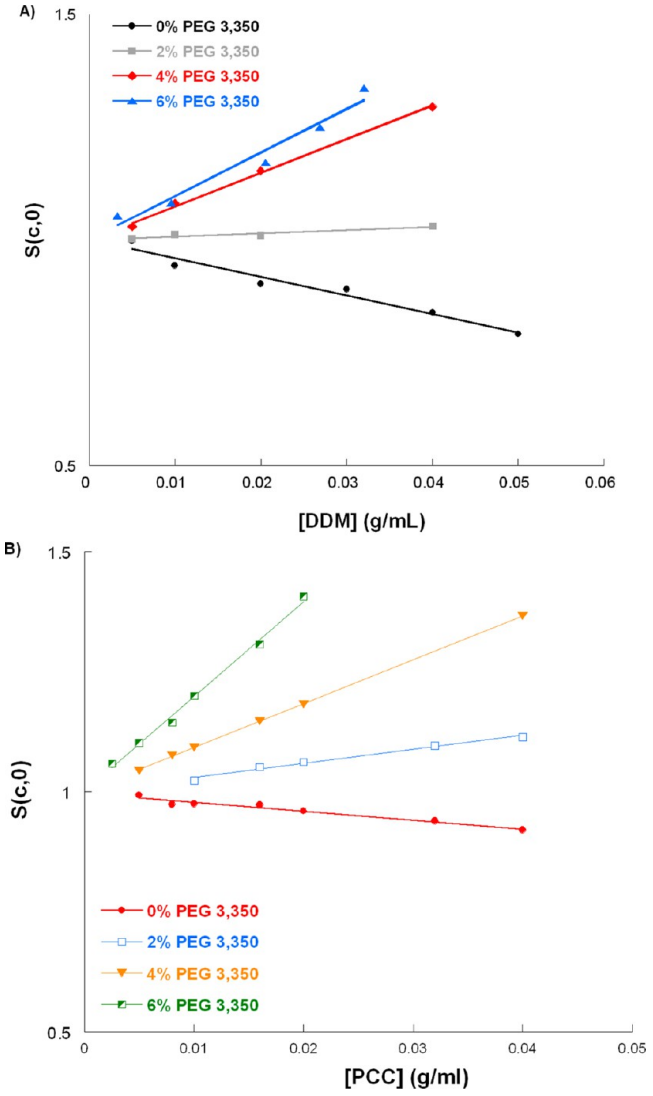

Figure 6. (A) DDβM and (B) PCCαM zero-q structure factor as a function of micelle concentration in different solutions Tris 20 mM pH 8 plus different percentage of PEG 3350.

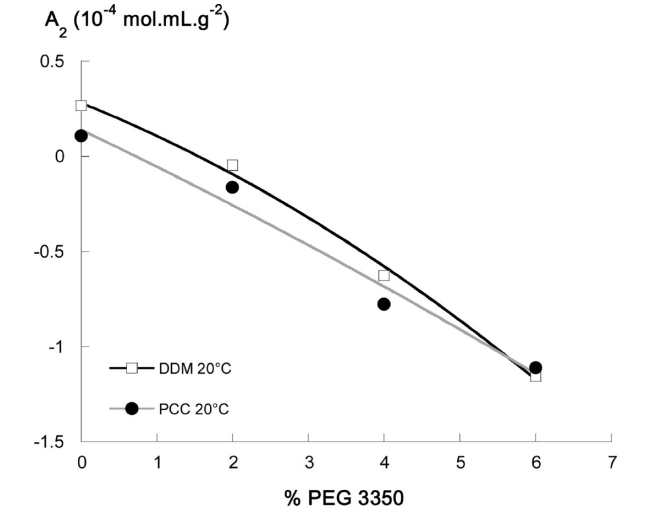

Figure 7. Second virial coefficients of DDβM and PCCαM micelles as a function of PEG 3350 percentage.

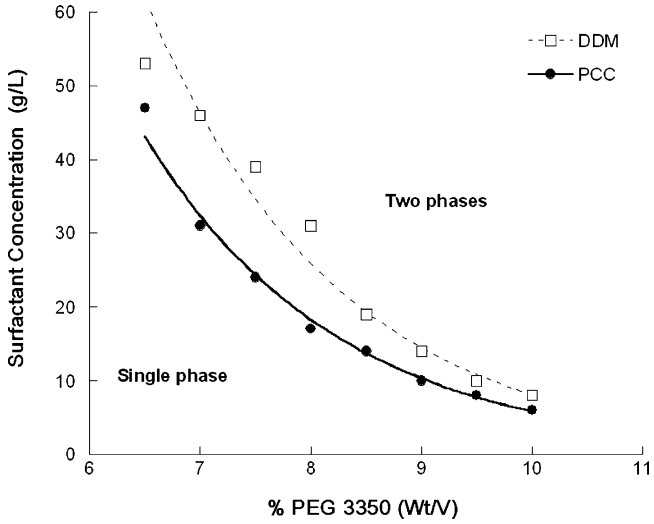

Figure 8. Phase transition map for DDβM and PCCαM micelles as a function of PEG 3350 percentages.

According to eq 10, the second virial coefficient (A_2), which reflects the overall interactions between particles in solution, has been plotted as a function of addition of PEG (Figure 7). It shows that, in solutions without PEG, PCCαM micelles are less repulsive than DDβM micelles in the same physicochemical conditions, i.e., $A_{2\ \mathrm{DD}\beta\mathrm{M}} > A_{2\ \mathrm{PCC}\alpha\mathrm{M}} > 0$. Since the two surfactants are non-ionic, repulsion between micelles is mainly due to micelle excluded volume effect. The discrepancy in A_2 between DDβM and PCCαM may be due to an increase in attractive interaction, probably to a modification in the van der Waals contribution in PCCαM micelles. We can expect that the anomeric form of PCCαM and its more rigid hydrophobic group favor the formation of denser and more packed micelles due to an increase in van der Waals contacts in the bulk of the micelle compared to the case of DDβM micelles, where the hydrophobic chains are more labile and present less van der Waals contacts. When PEG 3350 is added, up to 6%, forward scattering intensity increases as a function of micelle concentrations in the range [2.5−40 g·L^{-1}] (data not shown), without changes in the form factor in the large q-range. We have also observed that SAXS patterns of DDβM 40 g·L^{-1} at 6% PEG 3350 exhibited small diffraction peaks, whose signature led us to the formation of a hexagonal phase. When data are reported in zero-q structure factor as a function of micelle concentration, it shows that attractive interactions are induced when PEG is added and that PCCαM micelles are more attractive than DDβM micelles. This attraction between surfactant micelles in both cases in the presence of polymer is the well-known depletion attraction.[43] This depletion effect of polyethylene glycol is usual with proteins and was already observed with micelles of detergent.[15,44] The variation in the depletion effect is quite similar for DDβM and PCCαM (Figure 7).

However, with the supplementary attraction induced by PCCαM hydrophobic core, it may be possible that crystallization of integral membrane proteins purified in PCCαM should be favored at lower concentration of crystallizing agent.[14,17]

Surfactant Phase Map and RC-LH1-PufX Crystallization. Few articles in crystallography deal with the characterization of protein crystallization conditions via second virial coefficient determination. In the 2000s, Loll et al. first showed

dx.doi.org/10.1021/jp403483q | J. Phys. Chem. B 2013, 117, 8770−8781

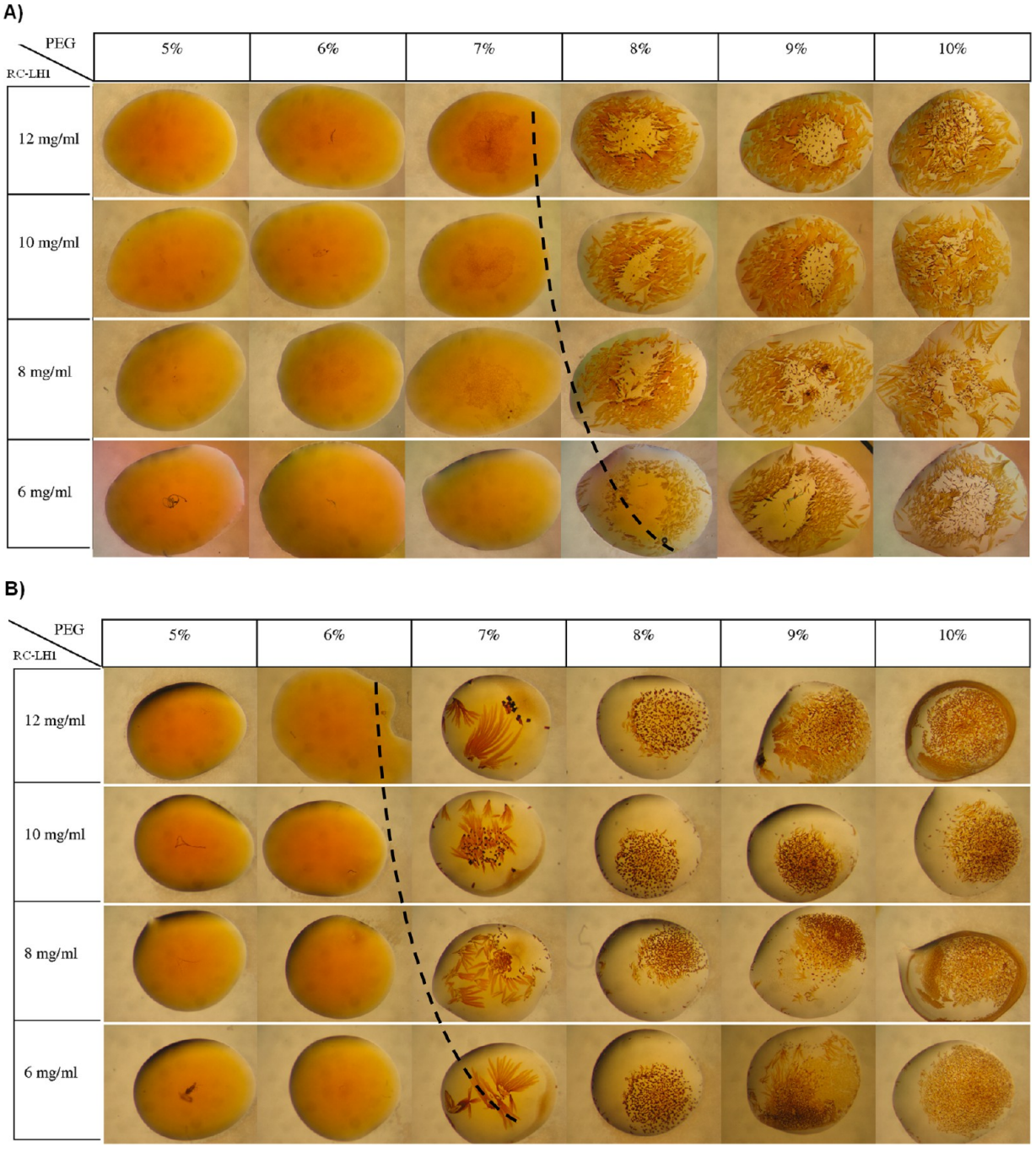

Figure 9. Crystallization trials of RC-LH1-PufX at 6, 8, 10, and 12 mg/mL with 5% to 10% PEG 3350 in vapor diffusion (concentrations are initial concentration prior mixing): (A) MP purified in DDβM, (B) MP purified in PCCαM.

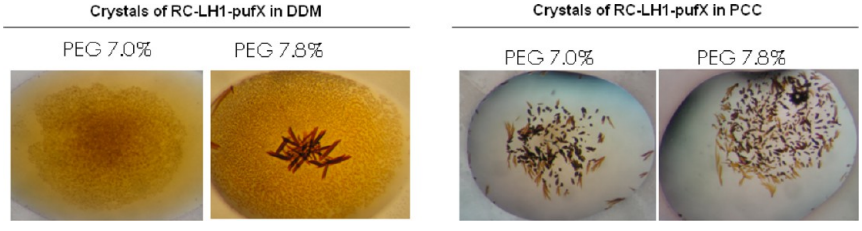

Figure 10. Crystals of RC-LH1-PufX in DDβM and PPCαM.

that, for integral membrane proteins, detergent (surfactant) moieties play an important role in modulating phase diagram of membrane protein detergent complexes (PDC) and that weak interaction forces between detergent micelles can be a predictive tool for the determination of PDC crystallization conditions. Conversely, could determination of attractive

dx.doi.org/10.1021/jp403483q | J. Phys. Chem. B 2013, 117, 8770−8781

interactions, via negative second virial coefficients, be an interesting alternative to empirical trial-and-error crystallization method for unknown MPs? We have shown here that micelles of PCCαM are more attractive than micelles of DDβM in the same crystallizing conditions. It is therefore expected that the surfactant phase diagram could be affected and that the cloud point boundary should be shifted toward lower polymer concentrations. This cloud point boundary, which corresponds to the condensation of micelles out of solution into a separate phase, has proven to be of interest in MP crystallization. Indeed, it has long been known that crystals of detergent-solubilized MPs tend to form near the cloud point of the detergent.[45] This empirical observation was used to construct crystallization screens, and a recent publication demonstrated that such screens could generate crystalline leads for over a dozen different membrane proteins.[46] We have thus observed by optical microscopy and drawn cloud point phase transitions of DDβM and PCCαM (Figure 8) and found that the cloud point for PCCαM is observed at lower percentage of PEG 3350 than in the case of DDβM.

This result suggests that crystallization of RC-LH1-PufX could occur at lower concentrations of crystallization agent when the membrane protein is purified in PCCαM compared to DDβM. Finally, crystallization trials, using the vapor diffusion method, have been performed with the RC-LH1-PufX complex purified in DDβM (0.015%) and PCCαM (0.010%). As observed on the two crystallization maps (Figure 9A and B), crystals of RC-LH1-PufX are observed in PCCαM at lower percentage of PEG 3350 after 7 days at 20 °C and lower concentration of the MP-surfactant complex, suggesting that its solubility curve is lower in PCCαM than in DDβM. This result is confirmed by optimization trials (Figure 10), which shows that, for identical percentages of PEG, solutions of RC-LH1-PufX are supersaturated in the presence of PCCαM than in DDβM. Crystals in PCCαM are more numerous and smaller than in DDβM.

This result clearly demonstrates that there is a close correlation between intermicellar interactions and crystallization of RC-LH1-PufX in surfactants, since no other parameter—buffer, salt, precipitant, crystallization method—has been modified. The question that remains is whether these crystals in this new surfactant diffract better. First trials do not show improvement in the diffraction quality. As we mentioned in the Introduction, detergent such as DDβM can destabilize membrane protein by intrusion of alkyl chains in the protein structure or by removing essential protein-bound lipids. It has recently been reported that adding phospholipids, which stabilizes MP structures, leads to MP crystals that diffract to better resolution. The nature and amount of phospholipids bound to RC-LH1-PufX have been characterized using a new high performance thin layer chromatography (HPTLC) assay.[47] It seems (Barret et al., personal communication) that when purified in PCCαM, RC-LH1-PufX associates 25% more phospholipids than when purified in DDβM. This result has to be correlated with the nondetergent effect of PCCαM and its higher hydrophobicity. Works are currently in progress to improve crystallization of RC-LH1-PufX in PCCαM and determine the amount and nature of phospholipids bound to the protein.

CONCLUSION

In this paper, we have compared micelle structure and intermicellar interactions of two mild surfactants, the classical dodecyl β maltoside and the derivative propyl(bi)cyclohexyl-α-maltoside in conditions used for membrane protein crystallization. We have first compared their structures in water by small-angle X-ray scattering complemented by gel permeation chromatography coupled to static light scattering. The surfactant micelle form factors are quite similar in shape but rather different in molar mass and aggregation number. We could fit SAXS experiments for both surfactants with a core−shell ellipsoid model. The PCC-α-maltoside appears a little larger but denser than DD-β-maltoside, which explains its more attractive behavior measured by second virial coefficients. A close correlation has been highlighted between higher attraction of micelles of PCCαM and lower cloud point boundary. Crystals of RC-LH1-PufX have finally been grown in PCCαM in conditions predicted by the surfactant phase diagrams. This work is pioneered in the crystallization field, by correlating modulation of surfactant structure hydrophobic moieties, particle interactions, and membrane protein crystallization. It opens ways for study of new amphiphilic molecules such as stabilizing fluorinated surfactants[48] not yet used for membrane protein crystallization.

AUTHOR INFORMATION

Corresponding Author

*E-mail: francoise.bonnete@univ-avignon.fr.

Notes

The authors declare no competing financial interest.

ACKNOWLEDGMENTS

This study was supported by a PhD grant from the region PACA (Provence Alpes Cote d'Azur-France) via FEDER funds. The SEC MALLS apparatus (from Wyatt Technology) was bought thanks to financial support from PACA, SANOFI-France, and Avignon University. We are grateful to the European Synchrotron Radiation Facility for provision of synchrotron radiation facilities and to Petra Pernot and Adam Round for assistance in using beamline ID14-eh3. We would like to thank Dr. Marina Siponen for diffraction tests and Thomas Zemb for fruitful discussion.

REFERENCES

(1) George, A.; Wilson, W. W. Predicting protein crystallization from a dilute solution property. *Acta Crystallogr.* **1994**, *D50*, 361−365.

(2) McMillan, W. G.; Mayer, J. E. The statistical thermodynamics of multicomponent systems. *J. Chem. Phys.* **1945**, *13*, 276−305.

(3) Zimm, B. H. Applications of the methods of molecular distribution to solutions of large molecules. *J. Chem. Phys.* **1946**, *14*, 164−179.

(4) Bonneté, F. Macromolecular crystallization controlled by colloidal interactions: the case of urate oxidase. In *Crystallization/Book 1* [Online] ; Andreeta, M. R. B., Ed.; Intech, 2012; Chapter 13; http://www.intechopen.com/books/crystallization-science-and-technology.

(5) Malfois, M.; Bonneté, F.; Belloni, L.; Tardieu, A. A model of attractive interactions to account for liquid-liquid phase separation of protein solutions. *J. Chem. Phys.* **1996**, *105* (B), 3290−3300.

(6) Tardieu, A.; Le Verge, A.; Riès-Kautt, M.; Malfois, M.; Bonneté, F.; Finet, S.; Belloni, L. Proteins in solution: from X-ray scattering intensities to interaction potentials. *J. Cryst. Growth* **1999**, *196*, 193−203.

(7) Vivares, D.; Belloni, L.; Tardieu, A.; Bonneté, F. Catching the PEG-induced attractive interaction between proteins. *Eur. Phys. J. E.* **2002**, *9*, 15−25.

(8) Guilloteau, J.-P.; Riès-Kautt, M. M.; Ducruix, A. F. Variation of lysozyme solubility as a function of temperature in the presence of organic and inorganic salts. *J. Cryst. Growth* **1992**, *122* (1−4), 223−230.
(9) Carbonnaux, C.; Riès-Kautt, M.; Ducruix, A. Relative effectiveness of various anions on the solubility of acidic Hypoderma lineatum collagenase at pH 7.2. *Protein Sci.* **1995**, *4* (10), 2123−8.
(10) Bonneté, F.; Finet, S.; Tardieu, A. Second virial coefficient: variations with lysozyme crystallization conditions. *J. Cryst. Growth* **1999**, *196*, 403−414.
(11) Vivarès, D.; Bonneté, F. X-ray scattering studies of Aspergillus flavus urate oxidase: towards a better understanding of PEG effects on the crystallization of large proteins. *Acta Crystallogr.* **2002**, *D58*, 472−479.
(12) Giffard, M.; Delfosse, V.; Sciara, G.; Mayer, C.; Cambillau, C.; El Hajji, M.; Castro, B.; Bonneté, F. Surfactant Poloxamer 188 as a New Crystallizing Agent for Urate Oxidase. *Cryst. Growth Des.* **2009**, *9*, 4199−4206.
(13) Hitscherich, C. J.; Kaplan, J.; Allaman, M.; Wiencek, J.; Loll, P. J. Static light scattering studies of OmpF porin: implications for integral membrane protein crystallization. *Protein Sci.* **2000**, *9*, 1559−1566.
(14) Hitscherich, C.; Aseyev, V.; Wiencek, J.; Loll, P. J. Effects of PEG on detergent micelles: implications for the crystallization of integral membrane proteins. *Acta Crystallogr.* **2001**, *D57*, 1020−1029.
(15) Loll, P.; Hitscherich, C.; Aseyev, V.; Allaman, M.; Wiencek, J. Assessing micellar interaction and growth in detergent solutions used to crystallize integral membrane proteins. *Cryst. Growth Des.* **2002**, *2* (6), 533−539.
(16) Berger, B. W.; Gendron, C. M.; Rlobinson, C. R.; Kaler, E. W.; Lenhoff, A. M. The role of protein and surfactant interactions in membrane-protein crystallization. *Acta Crystallogr.* **2005**, *D61*, 724−730.
(17) Berger, B. W.; Gendron, C. M.; Lenhoff, A. M.; Kaler, E. W. Effects of additives on surfactant phase behavior relevant to bacteriorhodopsin crystallization. *Protein Sci.* **2006**, *15* (12), 2682−2696.
(18) Berger, B. W.; Blamey, C. J.; Naik, U. P.; Bahnson, B. J.; Lenhoff, A. M. Roles of additives and precipitants in crystallization of calcium- and integrin-binding protein. *Cryst. Growth Des.* **2005**, *5* (4), 1499−1507.
(19) Prive, G. G. Detergents for the stabilization and crystallization of membrane proteins. *Methods: Structural Biology of Membrane Proteins* **2007**, *41* (4), 388−397.
(20) Wiener, M. C. A pedestrian guide to membrane protein crystallization. *Methods* **2004**, *34* (3), 364−372.
(21) Zhang, H.; Kurisu, G.; Smith, J. L.; Cramer, W. A. A defined protein-detergent-lipid complex for crystallization of integral membrane proteins: The cytochrome b6f complex of oxygenic photosynthesis. *Proc. Natl. Acad. Sci.* **2003**, *100* (9), 5160−5163.
(22) Park, K. H.; Berrier, C.; Lebaupain, F.; Pucci, B.; Popot, J. L.; Ghazi, A.; Zito, F. Fluorinated and hemifluorinated surfactants as alternatives to detergents for membrane protein cell-free synthesis. *Biochem. J.* **2007**, *403*, 183−187.
(23) Nehmé, R.; Joubert, O.; Bidet, M.; Lacombe, B.; Polidori, A.; Pucci, B.; Mus-Veteau, I. Stability study of the human G-protein coupled receptor, Smoothened. *Biochim. Biophys. Acta* **2010**, *1798* (6), 1100−1110.
(24) Duval-Terrié, C.; Cosette, P.; Molle, G.; Muller, G.; Dé, E. Amphiphilic biopolymers (amphibiopols) as new surfactants for membrane protein solubilization. *Protein Sci.* **2003**, *12* (4), 681−689.
(25) Yu, S. M.; McQuade, D. T.; Quinn, M. A.; Hackenberger, C. P. R.; Krebs, M. P.; Polans, A. S.; Gellman, S. H. An improved tripod amphiphile for membrane protein solubilization. *Protein Sci.* **2000**, *9* (12), 2518−2527.
(26) Tribet, C.; Audebert, R.; Popot, J. L. Amphipols: Polymers that keep membrane proteins soluble in aqueous solutions. *Proc. Natl. Acad. Sci. U.S.A.* **1996**, *93* (26), 15047−15050.
(27) Hovers, J.; Potschies, M.; Polidori, A.; Pucci, B.; Raynal, S.; Bonneté, F. o.; Serrano-Vega, M. J.; Tate, C. G.; Picot, D.; Pierre, Y.; Popot, J.-L.; Nehmé, R.; Bidet, M.; Mus-Veteau, I.; Bußkamp, H.; Jung, K.-H.; Marx, A.; Timmins, P. A.; Welte, W. A class of mild surfactants that keep integral membrane proteins water-soluble for functional studies and crystallization. *Mol. Membr. Biol.* **2011**, *28* (3), 171−181.
(28) Comayras, R.; Jungas, C.; Lavergne, J. Functional consequences of the organization of the photosynthetic apparatus in Rhodobacter sphaeroides - I. Quinone domains and excitation transfer in chromatophores and reaction center center dot antenna complexes. *J. Biol. Chem.* **2005**, *280* (12), 11203−11213.
(29) Konarev, P. V.; Volkov, V. V.; Sokolova, A. V.; Koch, M. H. J.; Svergun, D. I. PRIMUS: a Windows PC-based system for small-angle scattering data analysis. *J. Appl. Crystallogr.* **2003**, *36*, 1277−1282.
(30) Orthaber, D.; Bergmann, A.; Glatter, O. SAXS experiments on absolute scale with Kratky systems using water as a secondary standard. *J. Appl. Crystallogr.* **2000**, *33*, 218−225.
(31) Svergun, D. I. Determination of the Regularization Parameter in Indirect-Transform Methods Using Perceptual Criteria. *J. Appl. Crystallogr.* **1992**, *25*, 495−503.
(32) Kohlbrecher, J. *SASfit* v 0.93.3.
(33) Tanford, C. *The hydrophobic effect: Formation of micelles and biological membranes*; John Wiley & Sons, Inc.: New York, 1980; Vol. *18*, p 687.
(34) Israelachvili, J. N. *Intermolecular and surface forces*; Academic Press: Burlington, MA, 2011.
(35) Dupuy, C.; Auvray, X.; Petipas, C.; Rico-Lattes, I.; Lattes, A. Anomeric Effects on the Structure of Micelles of Alkyl Maltosides in Water. *Langmuir* **1997**, *13* (15), 3965−3967.
(36) Lipfert, J.; Columbus, L.; Chu, V. B.; Lesley, S. A.; Doniach, S. Size and shape of detergent micelles determined by small-angle x-ray scattering. *J. Phys. Chem. B* **2007**, *111* (43), 12427−12438.
(37) He, Z.; Garamus, V. M.; Funari, S. S.; Malfois, M.; Willumeit, R.; Niemeyer, B. Comparison of Small Angle scattering Methods for the structural analysis of Octyl-*β*-maltopyranoside micelles. *J. Phys. Chem. B* **2002**, *106*, 7596.
(38) Guinier, A.; Fournet, G. *Small angle scattering of X-rays*; Wiley: New York, 1955.
(39) Le Maire, M.; Champeil, P.; Møller, J. V. Interaction of membrane proteins and lipids with solubilizing detergents. *Biochim. Biophys. Acta* **2000**, *1508* (1−2), 86−111.
(40) Slotboom, D. J.; Duurkens, R. H.; Olieman, K.; Erkens, G. B. Static light scattering to characterize membrane proteins in detergent solution. *Methods* **2008**, *46* (2), 73−82.
(41) Fritz, G.; Bergmann, A. Interpretation of small-angle scattering data of inhomogeneous ellipsoids. *J. Appl. Crystallogr.* **2004**, *37*, 815−822.
(42) Bauer, C.; Bauduin, P.; Girard, L.; Diat, O.; Zemb, T. Hydration of sugar based surfactants under osmotic stress: A SAXS study. *Colloids Surf., A: Physicochem. Eng. Aspects* **2012**, *413*, 92−100.
(43) Asakura, S.; Oosawa, F. On the interaction between two bodies immersed in a solution of macromolecules. *J. Chem. Phys.* **1954**, *22*, 1255−1256.
(44) Tanaka, S.; Ataka, M.; Onuma, K.; Kubota, T. Rationalization of membrane protein crystallization with polyethylene glycol using a simple depletion model. *Biophys. J.* **2003**, *84*, 3299−3306.
(45) Wiener, M. C.; Snook, C. F. The development of membrane protein crystallization screens based upon detergent solution properties. *J. Cryst. Growth* **2001**, *232* (1−4), 426−431.
(46) Koszelak-Rosenblum, M.; Krol, A.; Mozumdar, N.; Wunsch, K.; Ferin, A.; Cook, E.; Veatch, C. K.; Nagel, R.; Luft, J. R.; DeTitta, G. T.; Malkowski, M. G. Determination and application of empirically derived detergent phase boundaries to effectively crystallize membrane proteins. *Protein Sci.* **2009**, *18* (9), 1828−1839.
(47) Barret, L.-A.; Polidori, A.; Bonneté, F.; Bernard-Savary, P.; Jungas, C. A new high-performance thin layer chromatography-based assay of detergents and surfactants commonly used in membrane protein studies. *J. Chromatogr., A* **2013**, *1281* (0), 135−141.
(48) Breyton, C.; Gabel, F.; Abla, M.; Pierre, Y.; Lebaupain, F.; Durand, G.; Popot, J. L.; Ebel, C.; Pucci, B. Micellar and Biochemical

Properties of (Hemi)Fluorinated Surfactants Are Controlled by the Size of the Polar Head. *Biophys. J.* **2009**, *97* (4), 1077−1086.